American Mineralogist, Volume 80, pages 1089–1092, 1995

Intracrystalline distribution of Ni in San Carlos olivine: An EXAFS study

LAURENCE GALOISY, GEORGES CALAS
Laboratoire de Minéralogie-Cristallographie, URA CNRS 09, Universités de Paris 6 et 7 et IPGP, 75252 Paris Cedex 05, France
GORDON E. BROWN, JR.
Department of Geological and Environmental Sciences and Stanford Synchrotron Radiation Laboratory, Stanford University, Stanford, California 94305-2115, U.S.A.

ABSTRACT

The location of minor amounts of Ni (0.44 wt% NiO) in the structure of San Carlos olivine has been determined using Ni *K*-edge fluorescence EXAFS spectroscopy. The mean Ni-O distance, d(Ni-O) = 2.08 Å, suggests a preferential location of Ni in the M1 site. The observed distance is smaller than the Mg-O distance in the M1 site of α-Mg_2SiO_4 [mean d(M1-O) = 2.10 Å] and is similar to the average M1-O distance in olivines close to the San Carlos composition [mean d(M1-O) = 2.09 Å]. The most important relaxation effect resulting from the Ni for Mg substitution is a smaller mean M1-O distance. The medium-range distribution of Ni (up to 4.5 Å from the central Ni atom) in the San Carlos olivine structure was estimated by modeling EXAFS spectra, considering various M1 and M2 cation distributions around M1 (Ni) sites. These models suggest medium-range ordering of Ni and Fe in adjacent M1 and M2 sites of the olivine structure and nonideal behavior of Ni in San Carlos olivine.

INTRODUCTION

The intracrystalline distributions of divalent cations in olivines have been widely investigated because of their potential use as geobarometers, geothermometers, and petrogenetic indicators (e.g., see Brown, 1982, for a review). The site preference of various first-row transition elements in olivines has been determined by X-ray diffraction (Rajamani et al., 1975; Boström, 1987), UV and visible spectroscopy (Burns, 1970), and Mössbauer spectroscopy (Annersten et al., 1982, 1984). Mg-, Fe-, and Ni-bearing olivines have received special attention because the partition coefficient of Ni between olivine and silicate melts has been used to model the generation and differentiation of mafic and ultramafic magmas (e.g., Hart and Davis, 1978; Kinzler et al., 1990). When Fe^{2+} is a major component of olivines, it is essentially randomly distributed between the two nonequivalent M1 and M2 octahedral sites (Burns, 1970; Brown and Prewitt, 1973; Nord et al., 1982). In contrast, Ni^{2+} and Co^{2+} preferentially occupy the M1 site (Rajamani et al., 1975; Walsh et al., 1976), and Mn^{2+} tends to prefer the M2 site (Annersten et al., 1982; Miller and Ribbe, 1985). However, because of the lack of sensitivity of the above-mentioned techniques, few attempts (e.g., Smyth and Tafto, 1982) have been made to verify the validity of this site-partitioning behavior for transition elements at trace levels in natural olivines.

Using the high sensitivity and chemical selectivity of fluorescence EXAFS (extended X-ray absorption fine structure) spectroscopy to overcome this difficulty, the strong M1 site preference of Ni^{2+} was determined in San Carlos olivine. EXAFS analysis revealed the presence of medium-range ordering of Ni and Fe in the San Carlos olivine structure in adjacent M1 and M2 sites, respectively.

EXPERIMENTAL METHODS

A green, translucent olivine sample from a spinel peridotite nodule (San Carlos, Arizona) was investigated. The identity of the sample was verified using X-ray diffraction. Electron microprobe analysis showed the presence of 0.44 wt% NiO, 0.50 wt% MnO, and 8.89 wt% FeO. EXAFS spectra of finely ground samples were collected at the Ni *K*-edge (8333 eV) at room temperature on wiggler beam line 4-3 at the Stanford Synchrotron Radiation Laboratory (SSRL, Stanford, California). Ring conditions were 3 GeV electron energy and 80–100 mA electron current. X-ray energy was monochromatized using Si(220) crystals detuned to avoid high-energy harmonics. The resulting energy resolution was ~1.9 eV. Energy was calibrated and checked before and after each scan using a copper metal foil and did not vary more than ±0.2 eV. Spectra were recorded over the energy range 8–9 keV using 0.1 eV steps in the edge region (8.30–8.35 keV) and 0.05 $Å^{-1}$ steps in the EXAFS region (8.35–9.0 keV) with a Ge array detector. The sample was mounted at 45° to the X-ray beam and the detector. Sintered α-Ni_2SiO_4 was used as a reference compound for comparison with the spectra from San Carlos olivine.

At the Ni *K*-edge energy, unwanted fluorescence from Fe hides the weak fluorescence from Ni and severely lim-

0003-004X/95/0910-1089$02.00

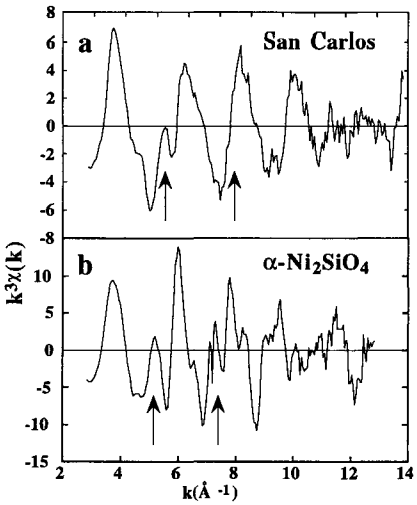

Fig. 1. Background-subtracted and normalized k^3-weighted EXAFS spectrum of Ni in (a) San Carlos olivine and (b) α-Ni_2SiO_4. The interference pattern due to the second-neighbor contribution to EXAFS is indicated by arrows.

its the utility of total fluorescence detection using conventional ion chambers. This difficulty was overcome using a Canberra 13-element Ge solid-state detector, which permits electronic discrimination against Fe $K\alpha$ and $K\beta$ fluorescence. The fluorescence EXAFS spectrum of Ni in San Carlos olivine (Fig. 1a) is the average of three spectra. The transmission EXAFS spectrum of α-Ni_2SiO_4 (Fig. 1b) was recorded under the same conditions as in previous EXAFS studies of Ni in glasses and crystals (Galoisy and Calas, 1993). Theoretical phase-shift and amplitude functions (McKale et al., 1988) were used in fitting both spectra. Data reduction was accomplished using a least-squares procedure previously described (Galoisy and Calas, 1991). A single and a double O shell around Ni were fit to both spectra to account for possible anharmonic effects resulting from O positional disorder. However, both the single and double O shell fits around Ni reproduced the mean Ni-O distance for α-Ni_2SiO_4 derived from X-ray diffraction. This observation, coupled with an analysis of possible anharmonic effects in α-Ni_2SiO_4 using the cumulant expansion approach (Jackson et al., in preparation), indicates that anharmonic effects are negligible. Accuracies of d(Ni-O) and d(Ni-Si) distances and Ni coordination number (N), based on similar EXAFS analysis of numerous model compounds, are ± 0.005, ± 0.02, and ± 0.5 Å atoms, respectively.

The cation distribution up to a 4 Å radius around Ni was modeled by simulating the Ni K-edge EXAFS spectrum of a $(Mg_{0.9}Fe_{0.1})_2SiO_4$ olivine (BFUNKI program: D. Bonnin, personal communication) using the interatomic distances determined by Birle et al. (1968) and theoretical McKale backscattering amplitude and phase-shift functions. The contribution of various atomic shells around Ni was considered in fitting the experimental San Carlos Ni spectrum. At this stage, however, it was not possible to distinguish between amplitude and phase-shift

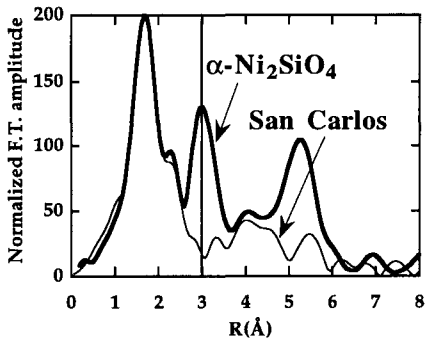

Fig. 2. Comparison of the normalized Fourier transforms of α-Ni_2SiO_4 and San Carlos olivine at the Ni K edge. The strong peak at 3 Å in α-Ni_2SiO_4 is indicated by a vertical line.

functions of Ni^{2+} and Fe^{2+} because these respective functions for Ni and Fe are quite similar. The σ^2 parameter was fixed at 0.01 $Å^2$ for all shells, except for the Si atoms belonging to the edge-sharing tetrahedra at 2.7 Å, for which a value of 0.006 $Å^2$ was taken. The λ was fixed at 2.2 $Å^{-2}$ for all shells.

Results

High-quality, low-noise, Ni K-edge X-ray absorption spectra of San Carlos olivine and α-Ni_2SiO_4 were obtained (Fig. 1). The absence of signal distortion at high photon energies allowed us to extract an EXAFS $\chi(k)$ signal up to 13 $Å^{-1}$. The complex shape of $\chi(k)$ is due to the contribution of the successive atomic shells around Ni. To derive the Fourier transform (F.T.), a Kaiser window from 3.4 to 12.4 $Å^{-1}$ with $\tau = 2.3$ was used. The peaks of the F.T. show the contributions of various atomic shells surrounding Ni (Fig. 2). The first peak represents O nearest neighbors at an apparent distance (uncorrected for phase shift) of 1.8 Å and corresponds to 5.9 ± 0.5 O atoms at d(Ni-O) = 2.08 ± 0.005 Å. The σ^2 value (0.005 $Å^2$) in San Carlos olivine is similar to that in α-Ni_2SiO_4 (0.006 $Å^2$), suggesting similar levels of positional disorder of the O shell around Ni. The shoulder on the major peak in the F.T. of San Carlos olivine corresponds to the contribution of Si second neighbors with a dervied Ni-Si distance of 2.70 Å. Because the major EXAFS contribution comes from the first-neighbor O shell, the Ni-Si distances may be extracted only by inverse Fourier transformation of the whole peak, including the shoulder, using the EXAFS parameters of the Ni-O pair. In contrast with α-Ni_2SiO_4, no major F.T. contribution appears beyond the Ni-Si correlation in San Carlos olivine, although several contributions from M1, M2, and farther Si neighbors are expected (Fig. 2). Such important differences between the two samples may arise only from differences in the cation distribution around Ni in San Carlos olivine.

Discussion

The site occupied by Ni in San Carlos olivine may be inferred by comparing EXAFS data and the structure of natural olivines. The mean Ni-O distance in San Carlos

olivine, 2.08 Å, is smaller than the mean M1-O and M2-O distances of synthetic α-Mg_2SiO_4, 2.09 and 2.13 Å, respectively (Fujino et al., 1981). In olivine of composition $(Mg_{0.9}Fe_{0.1})_2SiO_4$, which is assumed to be representative of San Carlos olivine, these distances are 2.10 and 2.14 Å, respectively (Birle et al., 1968). These comparisons strongly suggest that Ni is preferentially located in the M1 site in San Carlos olivine. This result is in agreement with previous results on natural or synthetic Ni-rich olivines, in which strong ordering of Ni on the M1 site was found (Rajamani et al., 1975; Bish, 1981; Miller and Ribbe, 1985). As $^{[6]}Ni^{2+}$ (r_{Ni} = 0.69 Å) is smaller than $^{[6]}Mg^{2+}$ (r_{Mg} = 0.72 Å) (Shannon, 1976), Ni should occupy the M1 site in preference to the larger M2 site. Fe^{2+} (r_{Fe} = 0.78 Å) is randomly distributed over both sites (Burns, 1993), whereas Mn^{2+} is preferentially located in the M2 site (r_{Mn} = 0.83 Å) (Michoulier et al., 1969; Smyth and Tafto, 1982). Both cation size and crystal-field effects are important in determining the intrasite distribution of Ni^{2+} in the olivine structure. The CFSE for Ni^{2+} is larger in the M1 site of olivine because of the smaller d(Ni-O) and hence higher value of the Δ parameter of the M1 site relative to M2.

Structural relaxation effects may explain the small observed size of the M1 sites occupied by Ni in San Carlos olivine, which is as small as the M1 site in α-Ni_2SiO_4 (Brown, 1982). A linear relationship is observed between $X_{Ni^{2+}}$ and d(Ni-O) values derived from X-ray diffraction in the olivines belonging to the Mg_2SiO_4-Ni_2SiO_4 solid-solution series (Fig. 3). The average d(Ni-O) found in San Carlos olivine, including experimental uncertainties, deviates from this general trend and is similar to that of the α-Ni_2SiO_4 end-member. This deviation suggests a structural relaxation of the M1 site around Ni impurities in an olivine close to the Mg_2SiO_4 composition. Such structural relaxation around trace elements cannot be observed with X-ray diffraction, which averages over all crystallographically equivalent sites in a structure irrespective of their possible compositional differences.

The observed relaxation can be understood by considering the information obtained from EXAFS about second neighbors around Ni. The point-group symmetry of the M1 site in $(Mg_{0.9}Fe_{0.1})_2SiO_4$ is approximately D_{4h} with four similar M1-O distances ($\approx$2.08 Å) and two longer ones (2.14 Å). The derived d(Ni-Si) in San Carlos olivine is 2.70 Å, which is slightly longer than the distance (2.68 Å) between edge-shared M1 octahedra and tetrahedra in α-Ni_2SiO_4 and the same as that in $(Mg_{0.9}Fe_{0.1})_2SiO_4$ (2.703 Å) (Brown, 1982). The similarity of d(Ni-Si) for San Carlos olivine and d(Mg-Si) for forsterite is somewhat surprising because the substitution of Ni^{2+} for Mg^{2+} should result in a shortening of this distance. A possible explanation for these results is that this substitution causes shortening of the two M1-O3 bonds and lengthening of the two M1-O2 bonds and the two M1-O1 bonds [to achieve the same $\langle d(M1\text{-}O)\rangle$ as in α-Ni_2SiO_4]. The M1-O3 and M1-O2 bonds are linked to the edge-shared SiO_4 tetrahedra, and so their changes in length owing to Ni substitution in M1 must be consistent with the observed d(Ni-Si) of 2.70 Å. These proposed changes should result in a more regular M1 site when it is occupied by Ni.

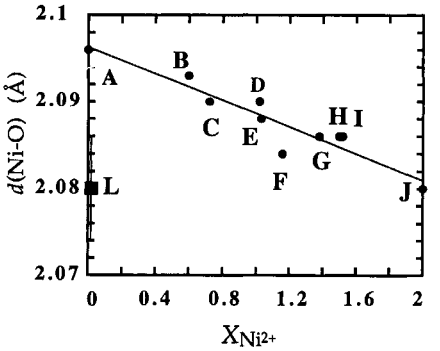

Fig. 3. Linear relationship between $X_{Ni^{2+}}$ and d(Ni-O) in various Mg- and Ni-containing olivines. The San Carlos sample in this study deviates from the general trend. Sample: A = Fujino et al. (1981); B, C, D, G, H, and J = Boström (1987); E = Rajamani et al. (1975); F and I = Bish (1981); L = San Carlos olivine, this study.

This structural relaxation around Ni was taken into account in the modeling of the environment of Ni in San Carlos olivine. EXAFS spectra were simulated using the experimental fits presented above for the two first shells and the d(Ni-M) distances of $(Mg_{0.9}Fe_{0.1})_2SiO_4$ olivine (Birle et al., 1968) for the further shells. Different M1 and M2 site populations were considered in this simulation, and all the EXAFS parameters were kept identical in all simulations. The most informative simulated F.T.s (Fig. 4) correspond to Mg atoms in M1 and M2 sites (Fig. 4a), Mg and Ni atoms in M1 and Mg in M2 (Fig. 4b), and Mg and Ni in M1 and Fe in M2 (Fig. 4c). Although amplitude and phase-shift functions cannot distinguish among transition elements such as Ni and Fe, the relaxation processes around Ni cause structural differences between these elements. The simulation in Figure 4a corresponds to a random distribution of Ni within the San Carlos olivine structure, i.e., a low probability of encountering another Ni atom close to a given Ni atom. An important feature is the appearance of a strong pair correlation at ~3.2 Å in the simulated F.T. because of the presence of the same atoms at similar Ni-M1 and Ni-M2 distances. A similar feature is found in the F.T. of α-Ni_2SiO_4 (Fig. 2) for the same reason. However, the intensity of this F.T. feature is smaller in the simulation in Figure 4a, which considers only Mg atoms, than observed in α-Ni_2SiO_4 because of the lower backscattering amplitude of Mg vs. Ni. The simulation in Figure 4b shows a modification of the shape of the 3 Å F.T. feature because of the phase difference between Mg and Ni. In the simulation in Figure 4c, the phase difference between Mg and Ni in the M1 sites and Fe in the M2 sites almost cancels the 3 Å peak in the F.T. This simulation gives a good fit of the experimental data. As mentioned above, no distinction between amplitude and phase-shift functions of Ni and Fe can be made. However, the good fit obtained

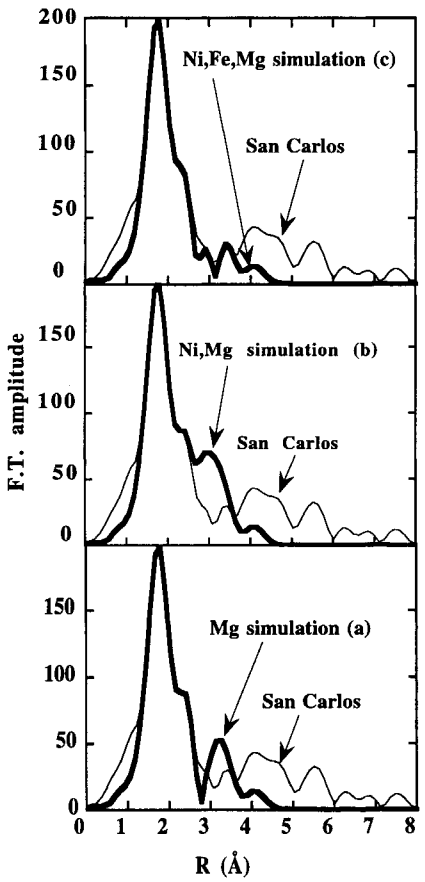

Fig. 4. (**a**) Simulations of the Fourier transform of the environment of Ni using the $(Mg_{0.9}Fe_{0.1})_2SiO_4$ structure. In **a**, only Mg atoms are assumed to occupy M1 and M2 around Ni; in **b**, Ni and Mg atoms are assumed to occupy M1 and Mg atoms to occupy M2 around Ni; in **c**, Ni and Mg atoms are assumed to occupy M1 and Fe atoms to occupy M2 around Ni.

in the 3 Å region of the F.T. is consistent with only Fe occupying the M2 sites around Ni. Thus, medium-range ordering of Ni,Fe in San Carlos olivine is indicated by comparison of the F.T.s of the experimental and simulated EXAFS spectra.

This preferential ordering of Ni in adjacent M1 sites suggests nonideal behavior of this element in San Carlos olivine. The relationship of these local concentrations of Ni to extended defects such as dislocations and growth rims must be clarified. The defect structure of natural olivines may play a role in the formation of these Ni- and Fe-enriched domains, which could be possible precursors of the precipitation of Fe-Ni metallic precipitates under reducing conditions previously observed in San Carlos olivine (Boland and Duba, 1986).

Acknowledgments

We are greatly indebted to R.C. Liebermann (SUNY Stony Brook), who kindly provided the San Carlos olivine sample, and to O. Jaoul (Orsay, France), who stressed the importance of the redox conditions on olivine properties. We also thank F. Farges (University of Marne-la-Vallée, France) for useful discussions. D. Bish (Los Alamos National Laboratory) and P. O'Day (Arizona State University) provided helpful comments on the manuscript. This work was supported by the NSF-CNRS Cooperative Program and by NSF (G.E.B.). SSRL is supported by the Department of Energy and the National Institute of Health.

References cited

Annersten, H., Ericsson, T., and Filippidis, A. (1982) Cation ordering in Ni-Fe olivines. American Mineralogist, 67, 1212–1217.

Annersten, H., Adetunji, J., and Filippidis, A. (1984) Cation ordering in Fe-Mn silicate olivines. American Mineralogist, 69, 1110–1115.

Birle, J.D., Gibbs, G.V., Moore, P.B., and Smith, J.V. (1968) Crystal structures of natural olivines. American Mineralogist, 53, 807–824.

Bish, D.L. (1981) Cation ordering in synthetic and natural Ni-Mg olivines. American Mineralogist, 66, 770–776.

Boland, J.N., and Duba, A.G. (1986) An electron microprobe study of the stability field and degree of non stoichiometry in olivine. Journal of Geophysical Research, 91(B5), 4711–4722.

Boström, D. (1987) Single-crystal X-ray diffraction studies of synthetic Ni-Mg olivine solid solutions. American Mineralogist, 72, 965–972.

Brown, G.E., Jr. (1982) Olivines and silicate spinels. In Mineralogical Society of America Reviews in Mineralogy, 5, 275–381.

Brown, G.E., Jr., and Prewitt, C.T. (1973) High-temperature crystal chemistry of hortonolite. American Mineralogist, 58, 577–587.

Burns, R.G. (1970) Crystal field spectra and evidence of cation ordering in olivine minerals. American Mineralogist, 55, 1608–1632.

——— (1993) Mineralogical applications of crystal field theory (2nd edition), 551 p. Cambridge University Press, Cambridge.

Fujino, K., Sasaki, S., Takeuchi, Y., and Sadanaga, R. (1981) X-ray determination of electron distributions in forsterite, fayalite, and tephroite. Acta Crystallographica, B37, 513–518.

Galoisy, L., and Calas, G. (1991) Spectroscopic evidence of five-coordinated Ni in $CaNiSi_2O_6$ glass. American Mineralogist, 76, 1777–1780.

——— (1993) Structural environment of nickel in silicate glass/melt systems: Part 1. Spectroscopic determination of coordination states. Geochimica et Cosmochimica Acta, 57, 3613–3625.

Hart, S.R., and Davis, K.E. (1978) Nickel partitioning between olivine and silicate melt. Earth and Planetary Science Letters, 40, 203–219.

Kinzler, R.J., Grove, T.L., and Recca, S.I. (1990) An experimental study on the effect of temperature and melt composition on the partitioning of nickel between olivine and silicate melt. Geochimica et Cosmochimica Acta, 54, 1255–1265.

McKale, A.G., Veal, B.W., Paulikas, A.P., Chan, S.K., and Knapp, G.S. (1988) Improved ab initio calculations of amplitude and phase functions for extended X-ray absorption fine structure spectroscopy. Journal of the American Chemical Society, 110, 3763–3768.

Michoulier, J., Gaite, J.M., and Maffeo, B. (1969) Résonance paramagnétique de l'ion Mn^{2+} dans un monocristal de forstérite. Comptes Rendus de l'Académie des Sciences de Paris, 269, 535–538.

Miller, M.L., and Ribbe, P.H. (1985) Methods for determination of composition and intracrystalline cation distribution in Fe-Mn and Fe-Ni silicate olivines. American Mineralogist, 70, 723–728.

Nord, A.G., Annersten, H., and Filippidis, A. (1982) The cation distribution in synthetic Mg-Fe-Ni olivines. American Mineralogist, 67, 1206–1211.

Rajamani, V., Brown, G.E., Jr., and Prewitt, C.T. (1975) Cation ordering in Ni-Mg olivine. American Mineralogist, 60, 292–299.

Shannon, R.D. (1976) Revised effective ionic radii and systematic studies of interatomic distances in halides and chalcogenides. Acta Crystallographica, A32, 751–767.

Smyth, J.R., and Tafto, J. (1982) Major and minor element site occupancies in heated natural forsterite. Geophysical Research Letters, 9(9), 1113–1116.

Walsh, D., Donnay, G., and Donnay, J.D.H. (1976) Ordering of transition metal ions in olivine. Canadian Mineralogist, 14, 149–150.

Manuscript received April 24, 1995
Manuscript accepted August 3, 1995